J|A|C|S
ARTICLES
Published on Web 08/24/2002

Helical Rosette Nanotubes with Tunable Chiroptical Properties

Hicham Fenniri,* Bo-Liang Deng, and Alexander E. Ribbe

Contribution from the 1393 H. C. Brown Chemistry Laboratory, Purdue University, West Lafayette, Indiana 47907-1393

Received March 11, 2002

Abstract: On the basis of transmission electron microscopy (TEM), dynamic light scattering (DLS), small-angle X-ray scattering (SAXS), and circular dichroism (CD) studies, compound **1** was shown to exist mainly in two states: (a) At high concentration ($\geq$1 mM, in methanol), **1** undergoes hierarchical self-assembly to generate rosette nanotubes with $\sim$4 nm diameter and a concentration-dependent hydrodynamic radius in the range 10−100 nm. Under these conditions, addition of a chiral amino acid promoter (L-Ala), that binds to the crown ether moiety of **1** via electrostatic interactions, promotes a rapid transition ($k_0 \approx 0.48\ s^{-1}$, for [**1**] = 0.046 mM, [L-Ala] = 2.8 mM) from racemic to chiral rosette nanotubes with predefined helicities as indicated by the resulting induced circular dichroism (ICD). (b) At low concentration ($\leq$0.04 mM, in methanol), **1** exists mainly in a nonassembled state as shown by TEM and DLS. Addition of L-Ala in this case triggers a relatively slow ($k_0 \approx 0.07\ s^{-1}$ for [**1**] = 0.04 mM, [L-Ala] = 2.4 mM) sequence of supramolecular reactions leading to the hierarchical self-assembly of rosette nanotubes with predefined helicities. Under both conditions a and b, the kinetic data unveiled the intrinsic ability of the rosette nanotubes to promote their own formation (autocatalysis). The degree of chiral induction was found to depend dramatically upon the chemical structure of the promoter. This process appears also to follow an all-or-none response, as the vast majority of the crown ether sites must be occupied with a promoter for a complete transition to chiral nanotubes to take place. Finally, both supramolecular pathways a and b offer an efficient approach for the preparation of helical rosette nanotubes with tunable chiroptical properties and may also be viewed as a process by which a predefined set of physical and chemical properties that characterizes a molecular promoter is expressed at the macromolecular level.

Nonrandom symmetry breaking in supramolecular systems may be induced by the following three general processes: (a) The sergeant and soldiers principle,[1] initially formulated for covalent polymeric systems[2] to describe the inductive effect of a small population of chiral components on the chiroptical outcome of macromolecular systems.[3] This effect was also recently reported as a means to transfer molecular chirality into oligomeric[4] systems as well as in a variety of supramolecular assemblies.[5] (b) Molecular recognition induced chirality, a well-studied phenomenon encountered in host−guest chemistry which ensues from the specific recognition of a chiral guest by an achiral host and can be rationalized on the basis of steric and electronic factors.[6] (c) External means such as chiral vortex forces,[7] photoinduced electron transfer,[8] and redox- and photoswitches.[8] A distinct advantage of these systems over those in which supramolecular chirality results from spontaneous resolution[9] is that the chiroptical outcome is predictable and reproducible. As a result, it can be utilized in chirotechnology[8] for the design of sensors,[3,6] chiral cholesteric phases,[6] catalysts,[10]

* To whom correspondence should be addressed. E-mail: hf@purdue.edu. Phone: (765) 494-5241. Fax: (765) 494-0239.

(1) (a) Green, M. M.; Peterson, N. C.; Sato, T.; Teramoto, A.; Cook, R.; Lifson, S. *Science* **1995**, *268*, 1860−1866. (b) Green, M. M.; Reiddy, M. P.; Johnson, R. J.; Darling, G.; O'Leary, D. J.; Wilson, G. *J. Am. Chem. Soc.* **1989**, *111*, 6452−6454.
(2) (a) Rowan, A. E.; Nolte, R. J. M. *Angew. Chem., Int. Ed.* **1998**, *37*, 63−68. (b) Ferringa, B. L.; van Delden, R. A. *Angew. Chem., Int. Ed.* **1999**, *38*, 3419−3438. (c) Yashima, E.; Matsushima, T.; Okamoto, Y. *J. Am. Chem. Soc.* **1997**, *119*, 6345−6359.
(3) (a) Akagi, K.; Piao, G.; Kaneko, S.; Sakamaki, S.; Shirakawa, H.; Kyotani, M. *Science* **1998**, *282*, 1683−1686. (b) Feringa, B. L.; Huck, N. P. M.; van Doren, H. A. *J. Am. Chem. Soc.* **1995**, *117*, 9929−9930. (c) Huck, N. P. M.; Jager, W. F.; de Lange, B.; Feringa, B. L. *Science* **1996**, *273*, 1686−1688. (d) Feringa, B. L.; Huck, N. P. M.; Schoevaars, A. M. *Adv. Mater.* **1996**, *8*, 681−684. (e) Seebach, D.; Beck, A. K.; Heckel, A. *Angew. Chem., Int. Ed.* **2001**, *40*, 93−138. (f) Oda, R.; Huc, I.; Schmutz, M.; Candau, S. J.; MacKintosh, F. C. *Nature* **1999**, *399*, 566−569. (g) Nakano, T.; Okamoto, Y. *Chem. Rev.* **2001**, *101*, 4013−4038. (h) Cornelissen, J. J. L. M.; Rowan, A. E.; Nolte, R. J. M.; Sommerdijk, N. A. J. M. *Chem. Rev.* **2001**, *101*, 4039−4070.
(4) (a) Prince, R. B.; Moore, J. S.; Brunsveld, L.; Meijer, E. W. *Chem.-Eur. J.* **2001**, *7*, 4150−4154. (b) Hill, D. J.; Mio, M. J.; Prince, R. B.; Hughes, T. S.; Moore, J. S. *Chem. Rev.* **2001**, *101*, 3893−4011.
(5) (a) Palmans, A. R. A.; Vekemans, J. A. J. M.; Havinga, E. E.; Meijer, E. W. *Angew. Chem., Int. Ed. Engl.* **1997**, *36*, 2648−2651. (b) Hirschberg, K. J. H. K.; Brunsveld, L.; Ramzi, A.; Vekemans, J. A. J. M.; Sijbesma, R. P.; Meijer, E. W. *Nature* **2000**, *407*, 167−170. (c) Brunsveld, L.; Lohmeijer, B. G. G.; Vekemans, J. A. J. M.; Meijer, E. W. *Chem. Commun.* **2000**, 2305−2306. (d) Prins, L. J.; Timmmerman, P.; Reinhoudt, D. N. *J. Am. Chem. Soc.* **2001**, *123*, 10153−10163. (e) Brunsveld, L.; Meijer, E. W.; Prince, R. B.; Moore, J. S. *J. Am. Chem. Soc.* **2001**, *123*, 7978−7984. (f) Prins, L. J.; De Jong, F.; Timmerman, P.; Reinhoudt, D. N. *Nature* **2000**, *408*, 181−184. (g) Brunsveld, L.; Folmer, B. J. B.; Meijer, E. W.; Sijbesma, R. P. *Chem. Rev.* **2001**, *101*, 4071−4097.
(6) (a) Tanatani, A.; Mio, M. J.; Moore, J. S. *J. Am. Chem. Soc.* **2001**, *123*, 1792−1793. (b) Borovkov, V. V.; Lintuluoto, J. M.; Inoue, Y. *J. Am. Chem. Soc.* **2001**, *123*, 2979−2989. (c) Rivera, J. M.; Craig, S. L.; Martin, T.; Rebek, J., Jr. *Angew. Chem., Int. Ed.* **2000**, *39*, 2130−2132. (d) Kikuchi, Y.; Kobayashi, K.; Aoyama, Y. *J. Am. Chem. Soc.* **1992**, *114*, 1351−1358.
(7) Ribó, J. M.; Crusats, J.; Sagués, F.; Claret, J.; Rubires, R. *Science* **2001**, *292*, 2063−2066.
(8) Canary, J. W.; Zahn, S. *Trends Biotechnol.* **2001**, *19*, 251−255.

10.1021/ja026164s CCC: $22.00

asymmetric synthesis of materials with electromagnetic and optoelectronic applications,[3a] information storage,[11] display systems,[3b−d] and photochromic materials,[12] and for the design of materials with unique chiral light-emitting and nonlinear optical properties.[13]

This report describes two supramolecular processes for the self-assembly of helical rosette nanotubes[14a] with adjustable chiroptical properties. The first is the result of symmetry breaking in a preexisting racemic mixture of M- and P-helical rosette nanotubes. The second is the result of the triggering effect of a chiral promoter on a prochiral molecular module that leads to the hierarchical self-assembly of the module−promoter complex into said rosette nanotubes. In both cases, the promoter assumes the dual role of transferring its molecular chirality, physical, and chemical properties to the supramolecular ensemble, and contributing to the stabilization of the resulting nanotubular assembly.

Induced Supramolecular Chirality in the Rosette Nanotubes. Although the naturally occurring guanosine 3′-monophosphate was proposed to form helical columnar stacks of hydrogen-bonded supermacrocycles (G-quartet) 40 years ago,[14b−d] it was not until the late 1980s and early 1990s that this supramolecular motif (broadly defined) was utilized to organize increasingly more sophisticated discrete assemblies in solution.[14e−m,15] One of the latest developments in this area consisted of the generation of self-assembled helical rosette nanotubes from low molecular weight synthetic modules in water.[14a] The heterobicyclic base **G**$_\wedge$**C** (Figure 1)[14a,16−18] has both the Watson−Crick H-bond donor−donor−acceptor of guanine and the Watson−Crick H-bond acceptor−acceptor−donor of cytosine. Because of the asymmetry of its hydrogen bonding arrays, their spatial arrangement, and the hydrophobic character of the bicyclic system, **G**$_\wedge$**C** undergoes a hierarchical self-assembly process in water to form a six-membered supermacrocycle maintained by 18 H-bonds (Figure 2, upper). The resulting and substantially more hydrophobic aggregate then undergoes a second level of organization to produce a tubular architecture defining an unoccluded central pore running the length of the stack (Figure 2, lower).

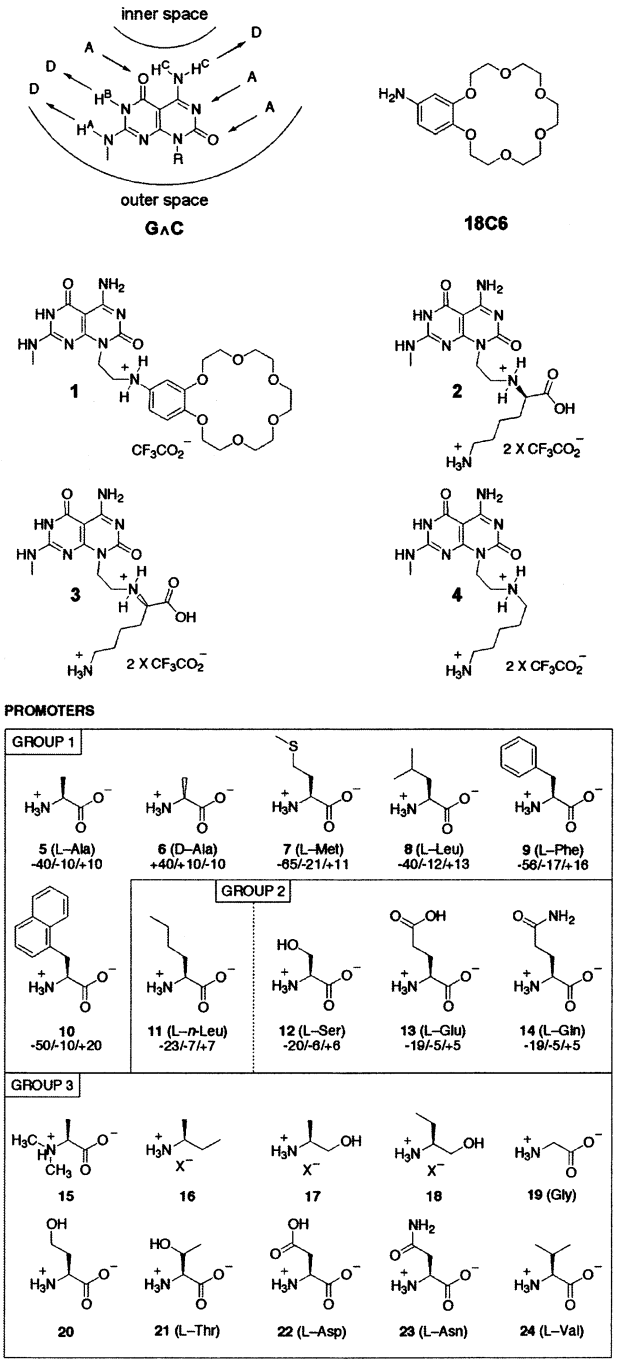

Figure 1. Nanotube-forming compounds (**1**−**4**) and promoters investigated. Groups 1 and 2 promoters induce supramolecular chirality, whereas group 3 does not. The numbers below the active promoters refer to the maximum induced ellipticity (in mDeg) at 237, 279, and 291 nm (237/279/291), for [**1**] = 0.04 mM and [promoter] = 0.4 mM. The CD spectra were recorded continuously until stabilization of the induced circular dichroism (ICD) (<24 h after mixing).[19]

Compound **1** (Figure 1), a conjugate of the **G**$_\wedge$**C** motif and 4-aminobenzo-18-crown-6-ether (18C6), was first investigated to establish the rosette nanotubes as stable, yet noncovalent scaffolds for the self-organization of multifunctional nanotubes in water (Figure 2).[18] We then went a step further toward modifying the nanotubes' physical and chemical properties by providing the crown ethers on their outer surface with unique

(9) (a) van Esch, J.; De Feyter, S.; Kellogg, R. M.; De Schrijver, F.; Ferringa, B. L. *Chem.-Eur. J.* **1997**, *3*, 1238−1243. (b) Takanishi, Y.; Takezoe, H.; Suzuki, Y.; Kibayashi, I.; Yajima, T.; Terada, M.; Mikami, K. *Angew. Chem., Int. Ed.* **1999**, *38*, 2354−2356. (c) Kirstein, S.; von Berlepsch, H.; Böttcher, C.; Burger, C.; Ouart, A.; Reck, G.; Dähne, S. *ChemPhysChem* **2000**, *3*, 146−150.
(10) Lorenzo, M. O.; Baddeley, C. J.; Muryn, C.; Raval, R. *Nature* **2000**, *404*, 376−379.
(11) Iftime, G.; Labarthet, F. L.; Natanshon, A.; Rochon, P. *J. Am. Chem. Soc.* **2000**, *122*, 12646−12650.
(12) Ichimura, K. *Chem. Rev.* **2000**, *100*, 1847−1873.
(13) (a) Kauranen, M.; Veerbiest, T.; Bouttoon, C.; Teerenstra, M. N.; Clays, K.; Schouten, A. J.; Nolte, R. J. M.; Persoons, A. *Science* **1995**, *270*, 966−969. (b) Verbiest, T.; Van Elshocht, S.; Kauranen, M.; Hellemans, L.; Snauwaert, J.; Nuckolls, C.; Katz, T. J.; Persoons, A. *Science* **1998**, *282*, 913−915.
(14) (a) Fenniri, H.; Mathivanan, P.; Vidale, K. L.; Sherman, D. M.; Hallenga, K.; Wood, K. V.; Stowell, J. G. *J. Am. Chem. Soc.* **2001**, *123*, 3854−3855. (b) Gellert, M.; Lipsett, M. N.; Davies, D. R. *Proc. Natl. Acad. Sci. U.S.A.* **1962**, *48*, 2013−2018. (c) Gotarelli, G.; Spada, G. P.; Garbesi, A. In *Comprehensive Supramolecular Chemistry: Templating, Self-Assembly, and Self-Organization*; Lehn, J.-M., MacNicol, D. D., Davies, J. A. D., Vogtle, F., Sauvage, J.-P., Hosseini, M. W., Eds.; Pegamon Press: Oxford, 1995; Vol. 9, pp 483−506. (d) Gilbert, D. E.; Feigon, J. *Curr. Opin. Struct. Biol.* **1999**, *9*, 305−314. (e) For a review, see: Lawrence, D. S.; Jiang, T.; Levett, M. *Chem. Rev.* **1995**, *95*, 2229−2260. (f) Ducharme, Y.; Wuest, J. D. *J. Org. Chem.* **1988**, *53*, 5787−5789. (g) Gallant, M.; Viet, M. T. P.; Wuest, J. D. *J. Org. Chem.* **1991**, *56*, 2284−2286. (h) Zerkowski, J. A.; Seto, C. T.; Whitesides, G. M. *J. Am. Chem. Soc.* **1992**, *114*, 5473−5475. (i) Zimmerman, S. C.; Duerr, B. F. *J. Org. Chem.* **1992**, *57*, 2215−2217. (j) Bonazzi, S.; De Morais, M. M.; Gottarelli, G.; Mariani, P.; Spada, G. P. *Angew. Chem., Int. Ed. Engl.* **1993**, *32*, 248−250. (k) Yang, J.; Marendaz, J.-L.; Geib, S.-J.; Hamilton, A. D. *Tetrahedron Lett.* **1994**, *35*, 3665−3668. (l) Russell, K. C.; Leize, E.; Van Dorsselaer, A.; Lehn, J.-M. *Angew. Chem., Int. Ed. Engl.* **1995**, *34*, 209−213. (m) Davis, J. T.; Tirumala, S.; Jenssen, J. R.; Radler, E.; Fabris, D. *J. Org. Chem.* **1995**, *60*, 4167−4176.

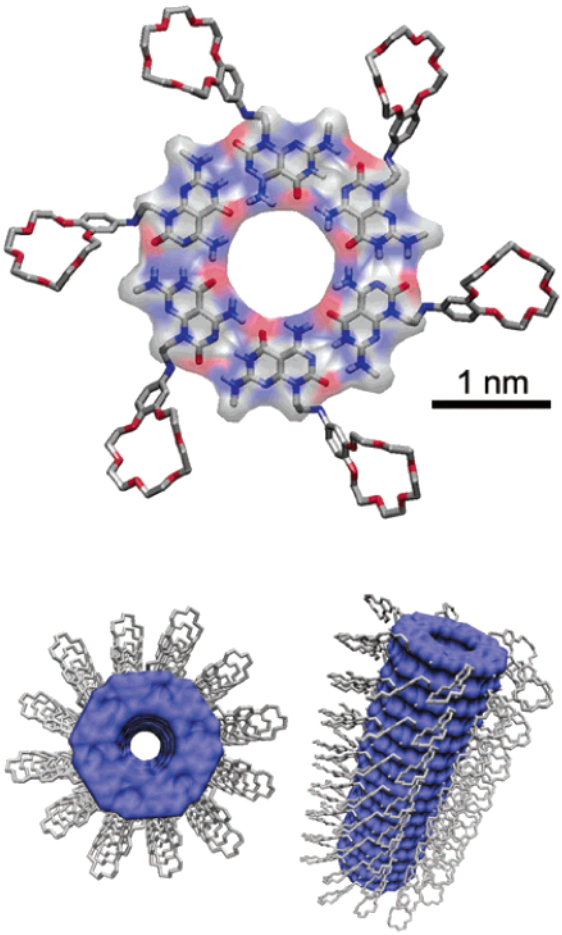

Figure 2. Hierarchical self-assembly of compound **1** into a six-membered supermacrocycle (rosette,[15−18] upper) and resulting nanotube, top (lower left) and side (lower right) views (Macromodel 7.2 and VMD).[19] Each crown ether site within the assembled structure provides 328 Å^3 of open space for binding of a molecular guest (e.g., promoters in Figure 1).

molecular guests.[20] We anticipated that such an interaction would impart reversible and predefined chemical and physical properties upon the nanotubular architectures. More specifically, an induced circular dichroism (ICD)[1−6] effect was expected to arise from the binding of a chiral amino acid in its zwitterionic

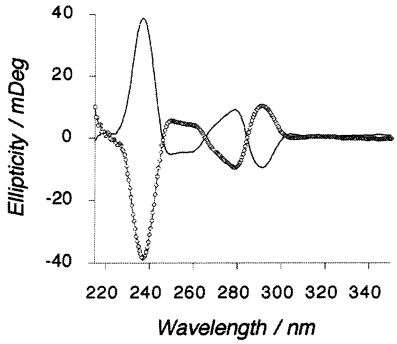

Figure 3. CD spectra of **1** (0.04 mM) + L-Ala (0.4 mM) (○) and **1** (0.04 mM) + D-Ala (0.4 mM) (−) recorded continuously until the induced circular dichroism (ICD) stabilized (<24 h after mixing).[19]

form to the prochiral crown ether-substituted derivative **1**. Indeed, in a methanolic solution, a typical CD spectrum[14a] was recorded in the presence of either L- or D-Ala (Figure 3). As control experiments, L-Ala, D-Ala, [L-Ala + 18C6], [D-Ala + 18C6], [**1** + D/L-Ala], 18C6, or **1** did not display any CD activity in the same wavelength range (200−350 nm, data not shown), whereas compounds **2** and **3**, featuring the $\mathbf{G}_{\wedge}\mathbf{C}$ motif covalently attached to L- and D-Lys, displayed identical CD spectral profiles.[14a]

Transmission electron microscopy (TEM, Figure 4B) and small-angle X-ray scattering (SAXS)[19] studies of concentrated samples of **1** (2.0 mM) in the absence of L-Ala confirmed the calculated tube diameter of ∼4 nm. The average hydrodynamic radius of the nanotubes (32.5 nm) derived from the dynamic light scattering (DLS) data (Figure 4A, curve #7) indicates that the nanotubes are composed on average of a stack of ∼140 rosettes (assuming 4.5 Å between stacks).[14a,18,19] The actual length is most likely larger, as the hydrodynamic radius defines a sphere in which the flexible assemblies are not necessarily perfectly linear. Evidence of the formation of the nanotubes in the presence of L-Ala was obtained from DLS (Figure 4A) and TEM (Figure 4C and D) studies. In conjunction with the CD investigations, these results demonstrated not only that the assembly does form in the presence of L-Ala at the micromolar concentrations required for CD measurements, but that this assembly is indeed expressing the molecular chirality of this promoter at the nanotubular level.

Generality of the Induced Supramolecular Chirality. To establish the generality of this process, we investigated 20 promoters (Figure 1). Three groups were identified on the basis of the amplitude of the ICD. The first group induced a strong CD signal (L-Ala, D-Ala, L-Met, L-Leu, L-Phe, **10**), the second induced a medium CD signal (L-*n*-Leu, L-Ser, L-Glu, L-Gln), and the third had no inductive effect (**15**−**18**, Gly, **20**, L-Thr, L-Asp, L-Asn, L-Val). Analysis of these data showed that: (a) All of the active promoters with the same chirality induce the same helicity. (b) Analogues of L-Ala (**15**−**18**), lacking the primary ammonium (**15**) or carboxylate function (**16**−**18**), did not induce any chirality. These functional groups are thus

(15) (a) Mathias, J. P.; Simanek, E. E.; Seto, C. T.; Whitesides, G. M. *J. Am. Chem. Soc.* **1993**, *115*, 1766−1769. (b) Seto, C. T.; Whitesides, G. M. *J. Am. Chem. Soc.* **1993**, *115*, 905−916. (c) Seto, C. T.; Mathias, J. P.; Whitesides, G. M. *J. Am. Chem. Soc.* **1993**, *115*, 1321−1329. (d) Seto, C. T.; Whitesides, G. M. *J. Am. Chem. Soc.* **1993**, *115*, 1330−1340. (e) Mathias, J. P.; Seto, C. T.; Simanek, E. E.; Whitesides, G. M. *J. Am. Chem. Soc.* **1994**, *116*, 1725−1736. (f) Mathias, J. P.; Simanek, E. E.; Whitesides, G. M. *J. Am. Chem. Soc.* **1994**, *116*, 4326−4340. (g) Simanek, E. E.; Qiao, S.; Choi, I. S.; Whitesides, G. M. *J. Org. Chem.* **1997**, *62*, 2619−2621. (h) Simanek, E. E.; Isaacs, L.; Li, X.; Wang, C. C. C.; Whitesides, G. M. *J. Org. Chem.* **1997**, *62*, 8994−9000. (i) Choi, I. S.; Li, X.; Simanek, E. E.; Akaba, R.; Whitesides, G. M. *Chem. Mater.* **1999**, *11*, 684−690. (j) Prins, L. J.; Timmerman, P.; Reinhoudt, D. N. *Pure Appl. Chem.* **1998**, *70*, 1459−1468. (k) Klok, H.-A.; Joliffe, K. A.; Schauer, C. A.; Prins, L. J.; Spatz, J. P.; Möller, M.; Timmerman, P.; Reinhoudt, D. N. *J. Am. Chem. Soc.* **1999**, *121*, 7154−7155. (l) Joliffe, K. A.; Timmerman, P.; Reinhoudt, D. N. *Angew. Chem., Int. Ed.* **1999**, *38*, 933−937. (m) Prins, L. J.; Thalacker, C.; Würthner, F.; Timmerman, P.; Reinhoudt, D. N. *Proc. Natl. Acad. Sci. U.S.A.* **2001**, *98*, 10042−10045. (n) Drain, C. M.; Russell, K. C.; Lehn, J.-M. *Chem. Commun.* **1996**, 337−338. (o) Krische, M. J.; Lehn, J.-M. *Struct. Bonding* **2000**, *96*, 3−29. (p) Kolotuchin, S. V.; Zimmerman, S. C. *J. Am. Chem. Soc.* **1998**, *120*, 9092−9093. (q) Sidorov, V.; Kotch, F. W.; Abdrakhmanova, G.; Mizani, R.; Fettinger, J. C.; Davis, J. T. *J. Am. Chem. Soc.* **2002**, *124*, 2267−2278.
(16) Marsh, A.; Silvestri, M.; Lehn, J.-M. *Chem. Commun.* **1996**, 1527−1528.
(17) Mascal, M.; Hext, N. M.; Warmuth, R.; Moore, M. H.; Turkenburg, J. P. *Angew. Chem., Int. Ed. Engl.* **1996**, *35*, 2204−2206.
(18) Fenniri, H.; Deng, B. L.; Ribbe, A. E.; Hallenga, K.; Jacob, J.; Thiyagarajan, P. *Proc. Natl. Acad. Sci. U.S.A.* **2002**, *99*, 6487−6492.
(19) See Supporting Information.
(20) (a) Izatt, R. M.; Pawlak, K.; Bradshaw, J. S. *Chem. Rev.* **1991**, *91*, 1721−2085 and refs 1 and 2 therein. (b) Gokel, G. *Crown Ethers and Cryptands*; The Royal Society of Chemistry: Cambridge, U.K., 1991. (c) Cooper, S R. *Crown Compounds: Toward Future Applications*; VCH Publishers: New York, 1992. (d) Dietrich, B.; Viout, P.; Lehn, J.-M. *Macrocyclic Chemistry: Aspects of Organic and Inorganic Supramolecular Chemistry*; VCH: Weinheim, Germany, 1993. (e) Al-Mustafa, J.; Hamzah, S.; Marji, D. *J. Solution Chem.* **2001**, *30*, 681−694.

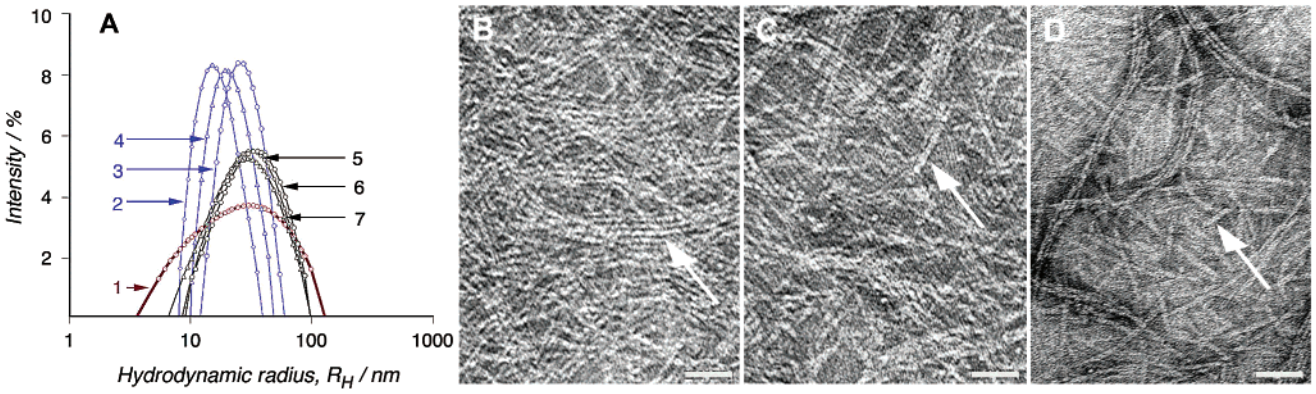

Figure 4. Dynamic light scattering (DLS) and transmission electron microscopy (TEM) studies of **1** in the absence and presence of L-Ala. (A) DLS regularization diagrams of **1** (0.04 mM) + L-Ala (0.4 mM) (curve #1); **1** (0.3 mM) + L-Ala (3.3 mM) (curve #2); **1** (1.0 mM) + L-Ala (1.0 mM) (curve #3); **1** (2.0 mM) + L-Ala (2.0 mM) (curve #4); **1** (0.3 mM) (curve #5); **1** (1.0 mM) (curve #6); **1** (2.0 mM) (curve #7). (B) TEM image of a negatively stained sample of **1** (2.0 mM in methanol). (C) TEM image of a negatively stained sample of **1** (0.3 mM) + L-Ala (3.3 mM). (D) TEM image of a negatively stained sample of **1** (0.04 mM) + L-Ala (0.4 mM). In the latter case, in the absence of L-Ala the nanotubes were undetectable by TEM and DLS.[19] The white arrows in B−D point at ~4 nm diameter rosette nanotubes. Scale bar = 25 nm.

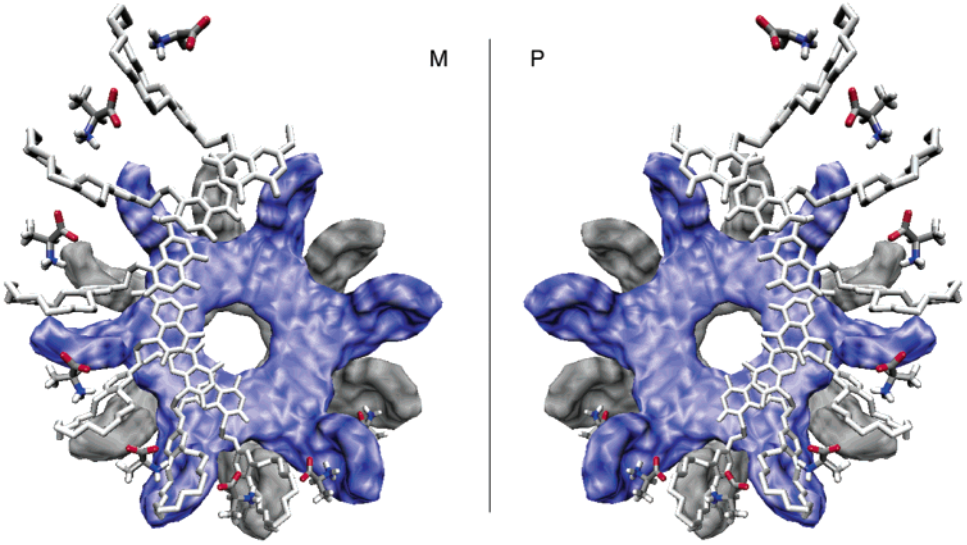

Figure 5. Docking of L-Ala/D-Ala promoters in M/P-helical nanotubes resulting from the hierarchical self-assembly of **1** (Macromodel 7.2 and VMD).[19] For clarity, the models show slightly tilted top perspective views with only one of the six noncovalent strands of the six-stranded rosette nanotubes (i.e., each self-assembling module **1** represents one rosette stack). For the side chains to point away from the walls of the nanotube and minimize steric hindrance, L-Ala and D-Ala must be fitted in M- and P-helical nanotubes, respectively. This model shows that the bound ammonium groups of each L-Ala amino acid are engaged in an additional electrostatic interaction with the carboxylate group of a neighboring L-Ala amino acid (from the staggered module situated 4.5 Å and ±30° below). This organization could result in a six-stranded helicoidal electrostatic belt composed of one-dimensional networks of amino acids (linked through electrostatic bonds) that wrap around and stabilize the rosette nanotubes.

essential for a promoter to induce supramolecular chirality and corroborate the proposed model of Figure 5. (c) The inductive effect is promoter-specific, and the binding of the promoter's ammonium group to the crown ethers is not the only factor determining the amplitude of the ICD. For instance, analogues of L-Ser (active), that differ with only a methylene (L-homoserine, **20**) or methyl group (L-Thr), did not induce any chirality. The same conclusion can be inferred from comparison of L-Glu/L-Gln (active) with L-Asp/L-Asn (inactive), or from comparison of L-Leu (active) with L-Val (inactive). The chiroptical outcome of the **1**−promoter complex within the supramolecular ensemble is therefore highly sensitive to minor structural variations. Except for L-Val and L-*n*-Leu, there appears to be a definite preference for small, aromatic, and hydrophobic amino acids, in agreement with the hydrophobic character of the methyl, phenyl, and crown ether groups lining up the six binding grooves of the rosette nanotubes. The case of L-Val may be rationalized on the basis of extensive steric hindrance near the promoter's anchor point (i.e., ammonium group) that may alter its binding properties.[20] The weak ICD of L-*n*-Leu, in comparison with the other hydrophobic promoters, could be related to the increased flexibility of its *n*-butyl side chain. (d) All active hydrophilic amino acids induce significantly weaker CD signals, most likely the result of a more pronounced interaction with the bulk polar solvent. (e) Achiral promoters have no inductive effect. In-depth molecular modeling studies are underway to rationalize this exquisite selectivity.

A promoter's inability to induce chirality can be due to destabilization of the nanotubes, lack of interaction, poor inducing power (unproductive fit), or the achiral nature of the promoter. In the latter two cases, the nanotubes may still be formed, and in fact TEM established that they do in the case of Gly.[19] In addition, DLS studies indicated that in the presence of a promoter, aggregation takes place regardless of the chemical

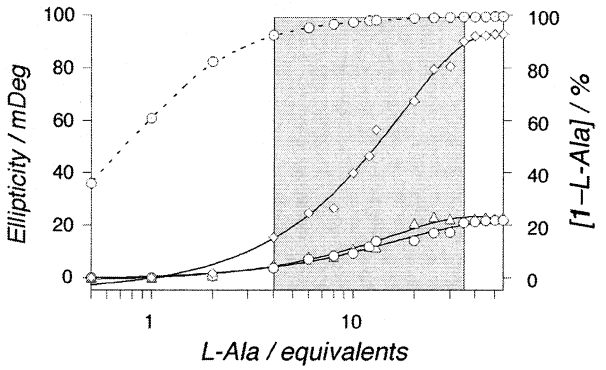

Figure 6. CD titration curve of **1** (0.04 mM) with L-Ala (1−55 equiv, left *Y* axis; ◊, 237 nm; ○, 279 nm; Δ, 291 nm), and (**1**−L-Ala) complex distribution as a function of [L-Ala] (⊙). The spectra were recorded continuously until the induced circular dichroism (ICD) stabilized (<24 h after mixing).[19] Analysis of the complex distribution versus ICD shows that the maximum induction is reached in a narrow window of complex (**1**−L-Ala) (93−99%) thereby revealing the all-or-none nature of this process.

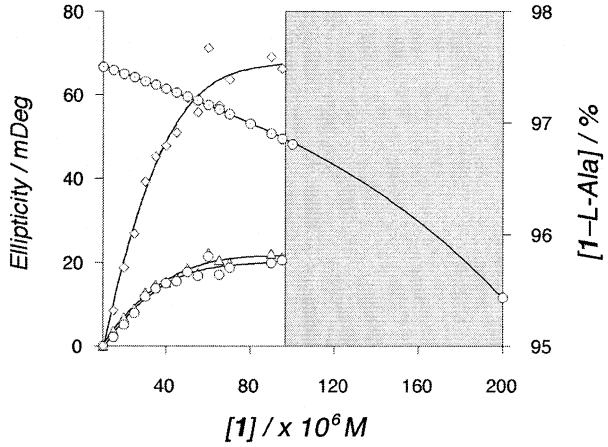

Figure 7. CD titration curve of L-Ala (0.4 mM) with **1** (0.01−0.09 mM) (left *Y* axis; ◊, 237 nm; ○, 279 nm; Δ, 291 nm), and (**1**−L-Ala) complex distribution curve (⊙) as a function of [**1**].[20] The spectra were recorded continuously until the ICD stabilized (<24 h after mixing).[19] Analysis of the (**1**−L-Ala) complex distribution curve versus ICD reveals that the latter increases as long as the concentration of the (**1**−L-Ala) complex is maximal (>97%). When the latter starts decreasing (<97%), the ICD levels out, in agreement with the proposed all-or-none response (see text).

nature of the promoter investigated as long as it possesses a primary ammonium and carboxylate functions (data not shown). In the absence of a promoter, however, the nanotubes disassemble at low concentration (0.04 mM). While these results, in conjunction with the CD studies, demonstrate that the chiroptical outcome is promoter-specific, it also reveals the generality of this supramolecular strategy as a means to stabilize and tailor the physical and chemical properties of the rosette nanotubes by simply selecting promoters offering the desired properties (e.g., charge, hydrophilicity, hydrophobicity, dipole, fluorescence).

All-or-None Nature of the Induced Supramolecular Chirality. The CD titration curve of **1** with L-Ala (Figure 6) revealed that the transition from racemic to helical rosette nanotubes takes place in the range of 4−30 equiv of L-Ala. On the basis of a conservative binding constant of $\sim 10^5$ of L-Ala to **1**,[19,20] this result suggests that the vast majority of the sites must be simultaneously occupied with an amino acid promoter for a complete transition to chiral nanotubes to take place (93−99%, Figure 6), despite the polydispersity of the sample ($5 < R_H < 100$ nm, Figure 4A, curve #1). From this observation, we concluded that the (**1**−L-Ala) complexes within the nanotubular assembly express their chirality collectively at the nanotubular level, but only when all of the crown ether sites are occupied with an amino acid (maximum site occupation requirement). This all-or-none response is at variance with a classical sergeant and soldiers mechanism,[1−5] in which a small chiral subpopulation determines the collective chiroptical destiny of the entire pool. The following additional experiments were carried out in support of this conclusion: (a) Addition of up to 1 equiv of **2** and **3**, which we had shown to result in optically active rosette nanotubes,[14a] to **1** and **4** (achiral, 0.04 mM) did not induce any supramolecular chirality. (b) Addition of up to 10 equiv of L-Ala to **4** (0.04 mM), which lacks the crown ether moiety, did not result in ICD. Similarly, addition of up to 10 equiv of *N*,*N*-dimethyl-L-Ala to the nanotubes resulting from **1** (0.04 mM) did not result in any CD activity. (c) Addition of 10 equiv of benzo-18-crown-6 (known to bind ammonium ions and amino acids)[20] to **1** (0.04 mM) and L-Ala (0.2 mM) resulted in complete suppression of the CD profile. (d) Addition of 10 equiv of glycine zwitterions (achiral) to **1** (0.04 mM) and L-Ala (0.2 mM) resulted in complete suppression of the CD profile. (e) Under typical sergeant and soldiers conditions, that is, L-Ala (0.01−0.04 mM) in the presence of a large excess of **1** (0.1−0.2 mM), conditions under which L-Ala is entirely in the bound state, did not result in any CD activity either. (f) Finally, titration of L-Ala (0.4 mM) with **1** (0.01−0.09 mM) results in a nonlinear increase of ICD that plateaus around 0.06 mM of **1** (Figure 7). Analysis of this curve in conjunction with the (**1**−L-Ala) complex distribution reveals that the ICD increases as long as the concentration of the (**1**−L-Ala) complex is maximal (>97%). When the latter starts decreasing (<97%), the ICD levels out, in agreement with the all-or-none nature of the induced supramolecular chirality. Note that the CD could not be recorded beyond 0.09 mM of **1** because of signal saturation, but judging from the titration profiles (Figures 6 and 7) and on the basis of the experiment e (above), the CD signal should vanish when the proportion of (**1**−L-Ala) complex falls below ~90%.

Taken together, these experiments not only support the proposed all-or-none response, but they also suggest that this could be the expression of a collective behavior involving all of the amino acids within the rosette nanotubes. Indeed, if we assume that the assemblies resulting from **1** are a 50/50 mixture of kinetically stable M and P nanotubes, the addition of L-Ala should not affect the chiroptical output of the mixture at least up to 50% (**1**−L-Ala) complex. That is, during the first half of the titration, L-Ala would preferentially bind to M-nanotubes, leaving the P-nanotubes unaltered. The second phase of the titration would require converting P-nanotubes into M-nanotubes, thereby unbalancing the P ↔ M equilibrium toward the latter and resulting in ICD. One can propose several possible pathways for this transition. The most likely one, in our opinion, that takes into consideration the above results as well as the experiments that will follow, would operate in a stepwise manner. We have established that a promoter imparts additional kinetic stability upon the nanotubes in which it fits best (vide infra). As a result, after saturating and stabilizing the M-nanotubes, L-Ala would bind to the P-nanotubes. However, because of an unfavorable fit with the latter, such an interaction would reduce their kinetic stability, possibly as a result of a

disordered and increased charge density. These destabilized P-nanotubes could then dissociate partially, and their components (rosettes, [**1**−L-Ala] complexes) could be recruited by the stabilized M-nanotubes via an "apparently" autocatalytic pathway (vide infra). If the destabilization put forward here requires a maximum occupation of the crown sites, it would provide a reasonable explanation for the all-or-none response. However, although the latter appears to be an experimental fact, further investigations are necessary to establish whether cooperativity plays a role in any part of this process.

Enantiospecificity, Reversibility, and Dominant/Recessive Behavior. The enantioselective nature of this process was readily demonstrated because all of the L-amino acids tested induced the exact opposite CD signature of their D-isomers, whereas achiral Gly did not induce any CD activity, as expected. For illustration, the spectra of L-Ala and D-Ala are shown in Figure 3. These results indicate that the ICD is not a random process, but rather the result of a specific interaction between the promoters and the self-assembled nanotubes.

The ICD resulting from a solution of **1** (0.04 mM) and L-Ala (0.4 M) was also reversibly abolished upon heating (Figure 8A). Heating the sample from 25 to 40 °C did not result in any change, whereas between 40 and 60 °C the ICD decreased steeply, in agreement with the observed all-or-none behavior. Temperatures above 60 °C were inaccessible due to the solvent used (methanol). Cooling down to room temperature restores 70% of the ICD within a few minutes and 100% within 24 h. Restoration of the ICD proceeds more or less rapidly depending on L-Ala's initial concentration. For instance, the presence of 50 equiv leads to complete restoration of the ICD within minutes of cooling to 25 °C. Also, the variable temperature CD profile shows five isosbectic points indicating that there are two main species in solution, and only one of them displaying supramolecular homochirality.

The inducing power of Ala is naturally proportional to its enantiomeric excess. Hence, the addition of a racemic mixture of Ala to the rosette nanotubes did not induce any CD activity, whereas 100% L-Ala induced the exact opposite spectrum of that obtained with 100% D-Ala (Figure 3). Remarkably, however, the addition of an excess of D-Ala (0.4 mM, 10 equiv) not only inverted the CD profile of a preequilibrated solution of **1** (0.04 mM) and L-Ala (0.2 mM, 5 equiv) (Figure 8B), but it did so as if L-Ala was not present in solution. That is, the intensity of the CD profile ended up being the same as that obtained for **1** (0.04 mM) and D-Ala (0.4 mM, 10 equiv) in the absence of any L-Ala (compare Figures 3 and 8B). This unexpected result suggests that the amino acid enantiomer present at higher concentration (D-Ala) not only binds to the nanotubes but apparently promotes the binding of its congeners and dictates the chirality outcome and its extent (*dominant* promoter), whereas L-Ala present in lower concentration (apparently) does not express its chirality at the supramolecular level (*recessive* promoter).

On the basis of the extent of ICD (Figure 8B), addition of the first 5 equiv of L-Ala resulted in a shift of the P ↔ M equilibrium toward 65% M-nanotubes. Addition of 10 equiv of D-Ala to this solution would capture the residual (nonconverted) P-nanotubes (35%) and starts competing with L-Ala for the M-nanotubes. Because D-Ala is present at higher concentration, it will naturally occupy more crown ether sites and help the system evolve toward more P-nanotubes according to the proposed autocatalytic mechanism (vide infra) and until it reaches a stationary phase defined by the titration curve of Figure 6. Besides demonstrating that the induction is reversible, this experiment suggests that the P ↔ M equilibrium is driven toward its stationary phase by the self-seeding helical nanotube present in higher concentration, which is determined by the amino acid enantiomer present at the highest concentration. This result suggests also that the amino acids within their sterically matching nanotubes must interact cooperatively not only to stabilize but also to feed their nanotube host with additional rosette stacks and (**1**−promoter) complexes. We propose that this interaction materializes in the form of electrostatic bonds between carboxylate and ammonium groups as shown in the model of Figure 5.

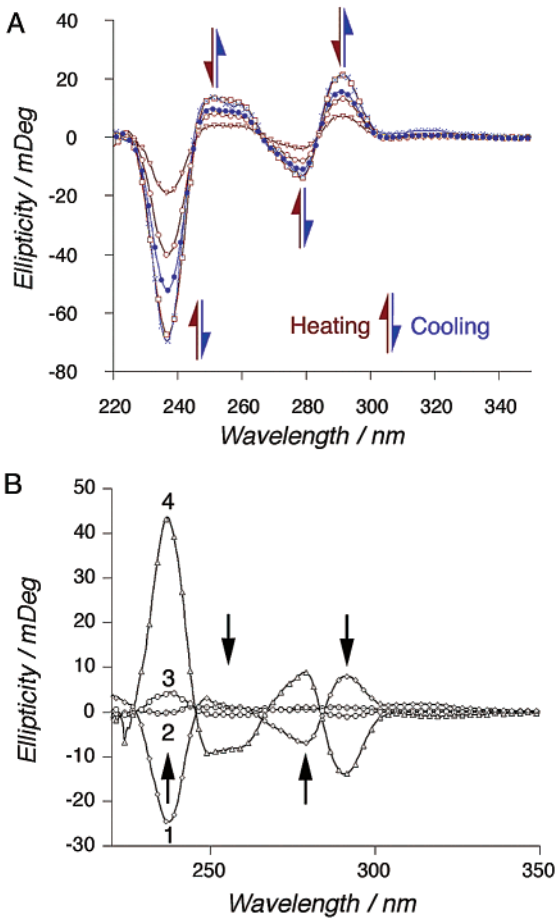

Figure 8. (A) Variable temperature CD of a solution of 1 (0.04 mM) + L-Ala (15 equiv) showing the reversible nature of the ICD. The temperature of 60 °C was not exceeded because of the solvent used (methanol). The red spectra were recorded at 25 °C (□), 40 °C (□), 50 °C (○), and 60 °C (▽). The blue spectra were recorded immediately after cooling (●) and 24 h later (×) (T_{ramp} = 1 °C/min).[19] (B) CD spectrum of a solution of **1** (0.044 mM, final concentration) and L-Ala (0.222 mM, final concentration), spectrum #1. Addition of D-Ala (0.4 mM, final concentration), which reduces the concentration of 1 and L-Ala to 0.04 mM and 0.2 mM, respectively, leads to a time-dependent and complete inversion of the CD profile (spectrum #2, t = 0 h; spectrum #3, t = 3 h; spectrum #4, t = 528 h). Note that the amplitude of spectrum #4 is close to that of **1** (0.04 mM) and D-Ala (0.4 mM) in the absence of L-Ala (see Figure 3), thereby revealing the dominant/recessive behavior of the promoters (see main text).

Supramolecular Pathways Leading to the Helical Rosette Nanotubes. In the process of investigating the concentration dependence of the ICD, we uncovered the following key

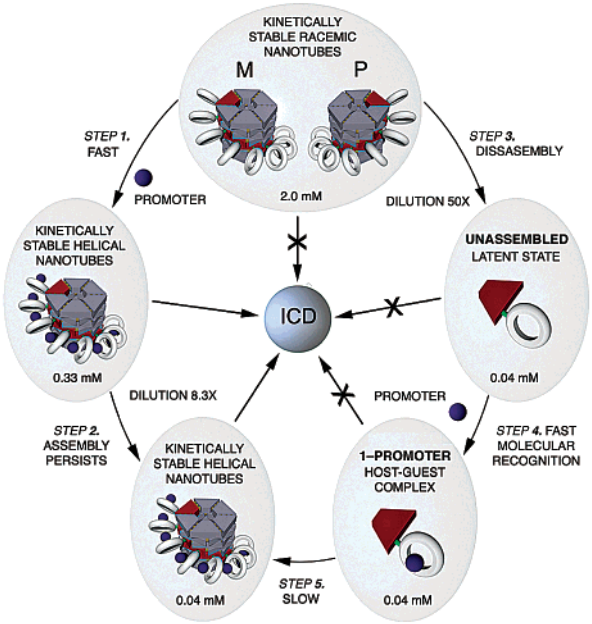

Figure 9. Schematic representation of the supramolecular pathways leading to the self-assembly of helical rosette nanotubes with tunable chiroptical properties. The fast pathway (steps 1 and 2) involves premixing concentrated solutions of **1** (2.0 mM) and L-Ala (4.0 mM) prior to dilution to the desired concentration. The slow pathway (steps 3−5) involves prediluting the stock solution of **1** (to 0.04 mM) prior to adding L-Ala (10 equiv).[19] Each of the five circles defines a state that was established by TEM, DLS, CD spectroscopy and/or kinetic studies (see main text). Steps 1 and 2 show that the nanotubes are kinetically stable in the presence of a promoter, and steps 3−5 show that the formation of the nanotubes can be triggered with a promoter. Both pathways lead to the helical rosette nanotubes.

features: (a) Premixing concentrated stock solutions of **1** (2 mM) and L-Ala prior to dilution in methanol results in an instantaneous ICD that rapidly reaches its maximum[21,22] (e.g., within seconds[21,23] in the presence of 50 equiv of L-Ala). This is schematically represented as the *fast* supramolecular pathway (Figure 9, steps 1 and 2). Interestingly, despite the 50-fold dilution (from 2.0 to 0.04 mM, Figure 9, steps 1 and 2), the nanotubes were still present as shown by DLS (Figure 4A, curves #7 and #1) and TEM (Figure 4B−D). (b) Adding **1** (0.04 mM, final concentration) to a prediluted solution of L-Ala (50 equiv) in methanol resulted in immediate ICD that reached its maximum within minutes (Figure 10A). (c) In contrast with (a) and (b), diluting the stock solution of **1** in methanol prior to adding the promoter does not result in any CD activity (Figure 9, step 3). DLS and TEM studies confirmed that there was no aggregation without L-Ala. Addition of L-Ala (10 equiv) to this solution leads to rapid host−guest complex formation[20] (Figure 9, step 4), triggers the self-assembly process, and results in a typical ICD profile that builds up over several hours (Figure 9, step 5, see also Figure 10C).[21,24] From this sequence of experiments (a−c), it appears that diluting **1** in its assembled state (i.e., from a concentrated solution) into a solution containing L-Ala leads to instantaneous formation and stabilization of the resulting chiral nanotubes, whereas in the absence of L-Ala the nanotubes disassemble at low concentration (kinetically unstable). Addition of L-Ala in the latter case results in the

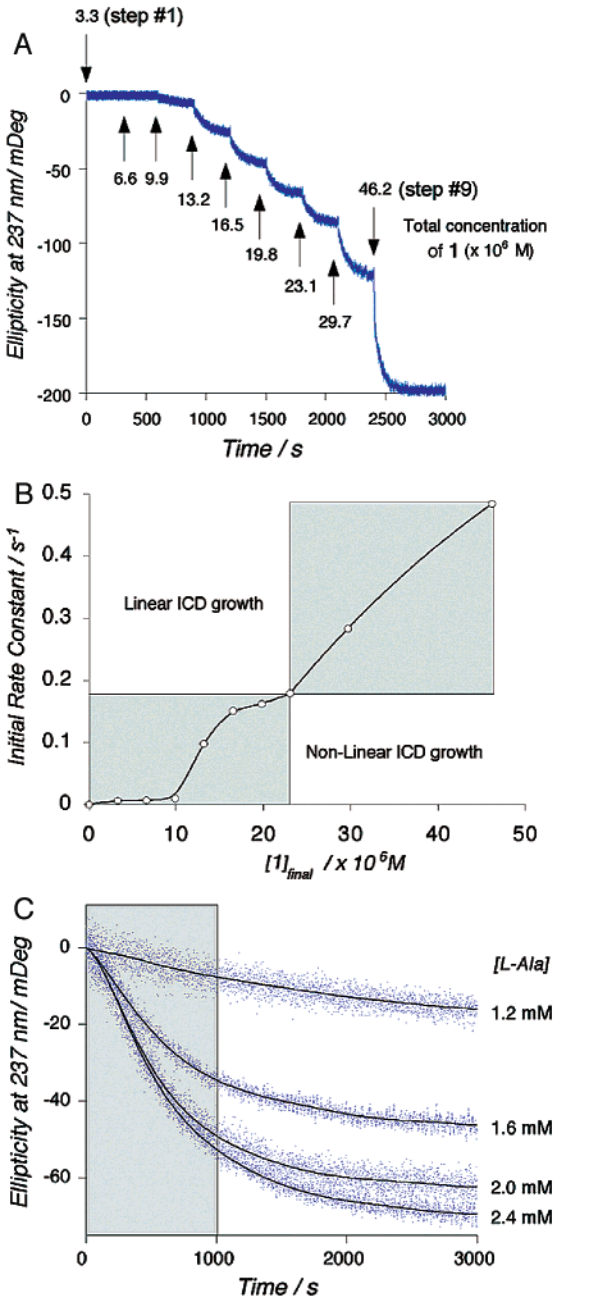

Figure 10. (A) Kinetics of the fast supramolecular pathway involving preassembled **1** (Figure 9, steps 1 and 2). The ICD grows as a result of incremental additions of a 2.0 mM stock solution of **1** to a 2.8 mM solution of L-Ala. The overall concentration of **1** after each increment is indicated above/below each arrow. From increments 1 to 7 (0.0033−0.0231 mM), the ICD grows nonlinearly as shown in plot B. (B) Observed initial rate constants of ICD growth derived from plot A as a function of the final concentration of **1**, showing a sigmoidal induction phase (steps 1−7) followed by a linear behavior (steps 7−9), suggesting that the nanotubes promote their own formation. (C) Kinetics of the slow supramolecular pathway involving unassembled **1** (Figure 9, steps 3−5). The sigmoidal growth of the ICD (gray box) resulting from the addition of various concentrations of L-Ala (1.2−2.4 mM) to **1** (0.04 mM) suggests here again that the nanotubes promote their own formation. Note that at the low concentration of **1** used in this experiment, the nanotubes are not preassembled. As a result, L-Ala acts as a chirality inducer and a trigger of the self-assembly process.[19]

(21) Concentration of stock solutions in methanol [**1**] = 2.0 mM, [L-Ala] = 4.0 mM.
(22) Concentrations prior to dilution in methanol [**1**] = 0.333 mM, [L-Ala] = 3.333 mM. Concentrations after dilution in methanol [**1**] = 0.04 mM, [L-Ala] = 0.4 mM.
(23) Concentrations prior to dilution in methanol [**1**] = 0.077 mM, [L-Ala] = 3.85 mM. Concentrations after dilution in methanol [**1**] = 0.04 mM, [L-Ala] = 2.0 mM.
(24) Concentrations of L-Ala prior to addition of **1**, [L-Ala] = 0.392 mM (10 equiv) and 1.96 mM (50 equiv). Concentrations of L-Ala and **1** after addition of **1**, [**1**] = 0.04 mM, [L-Ala] = 0.4 mM (10 equiv) and 2 mM (50 equiv).

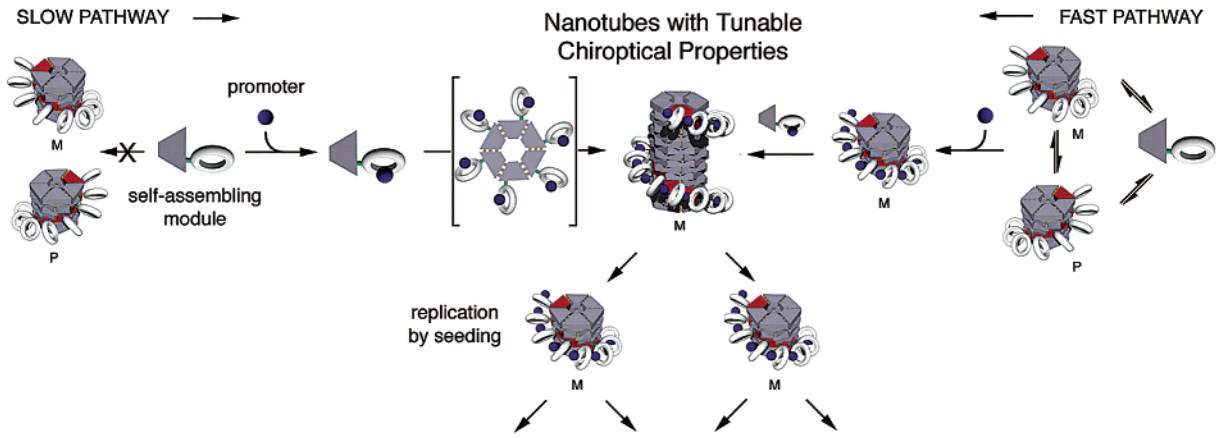

Figure 11. Supramolecular pathways and their proposed autocatalytic nature for the formation of helical rosette nanotubes with predefined properties.

instanteneous[20] formation of (**1**−L-Ala) host−guest complex and triggers the self-assembly of the helical rosette nanotubes. Because no aggregates were detected by TEM and DLS in the absence of L-Ala, we concluded that the latter contributes substantially to the stabilization of the final assembly (thermodynamic product). Comparison of the *fast* with the *slow* supramolecular pathways suggests also that the nanotubes are kinetically stable in the presence of a promoter, even at low concentration (0.04 mM).

The origin of the fast and slow supramolecular pathways is multifold: First, addition of L-Ala to preformed P/M nanotubes results in the immediate and stereoselective binding to one of the helical isomers, thereby shifting the P ↔ M equilibrium toward the formation of homochiral nanotubes as proposed above. From (a)−(c) (previous section), we inferred that at low concentration of **1**, the presence or absence of the promoter determines, respectively, whether the nanotubes will form or not. It is reasonable, therefore, to consider that without a promoter, **1** exists in a latent state, in which the crowns could interact intramolecularly with the **G**$_\wedge$**C** bases via H-bonds, thereby preventing them from undergoing the self-assembly process. Addition of L-Ala that binds to the crown moiety would, as a result, not only unleash the **G**$_\wedge$**C** base but also provide a thermodynamically favorable pathway for self-assembly through the stabilization of the resulting nanotubes. Through their hydrophobic ends ("binding sites"), these selectively stabilized nanotubes then provide new platforms for stereoselective growth. That is, the recruiting of additional rosette stacks or (**1**−L-Ala) complexes would extend the nanotubes, which upon random fracturing into shorter nanotubes would provide new "autocatalytic" pathways for elongation and multiplication, as suggested above. This self-seeding mechanism, summarized in Figure 11, provides a reasonable explanation for the following kinetics.

The kinetics of Figure 10A and B were conducted under saturating concentration of L-Ala and, as a result, saturating concentration of (**1**−L-Ala) complex. The concentration of the stock solution of **1** was chosen to ensure the preexistence of the nanotubes (2.0 mM). Incremental addition of the latter solution to L-Ala (2.8 mM) resulted initially in marginal ICD (steps 1−3), then in a substantial increase in ICD (step 4). Beyond the fourth increment, the ICD recorded and initial rate constant associated with it became directly proportional to the concentration of **1**. The weak ICD of increments 1−3 could be due to partial disassembly of the nanotubes as a result of the final low concentration of **1** in the reaction mixture. The fourth increment of preassembled nanotubes most likely acts as a catalyst to promote the assembly of the preexisting pool of unassembled (**1**−L-Ala) complexes, thereby resulting in increased initial rates and ICD ($k_0 \approx 0.48$ s^{-1} for [**1**] = 0.046 mM and [L-Ala] = 2.8 mM). The kinetics of Figure 10C were conducted under the conditions where **1** is not preassembled. Addition of L-Ala to this solution triggers a slow and sigmoidal growth of the ICD during the initial phase of the process ($k_0 \approx 0.07$ s^{-1} for [**1**] = 0.04 mM and [L-Ala] = 2.4 mM). Thus, it is clear from (a) the nonlinear dependence of the ICD (Figure 10A) and initial velocity (Figure 10B) on the initial concentration of **1** (Figure 10A, steps 1−7), and (b) the sigmoidal growth of the ICD versus time during the initial phase of the reaction between unassembled **1** and L-Ala (Figure 10C), that autocatalysis[25] may indeed play a significant role in this process. Detailed kinetic investigations and structural analogues studies are underway to firmly establish these observations, and also to provide a mathematical model for similar systems such as the self-assembly and replication of the prion protein.[26]

Conclusion

Expression of molecular chirality at the macromolecular level through self-assembly and self-organization is a topic of immense current interest.[1−9,14a] It may lead not only to a better understanding of nature's approach to generating supramolecular architectures with predefined size, topology, stereochemistry, hierarchy, and shape, but also to numerous technological applications.[3a−d,8−13] Here we report on a system wherein molecular chirality is expressed at the macromolecular level via two hierarchical processes. At millimolar concentration, **1** self-assembles into a racemic mixture of left (M)- and right (P)-handed helical rosette nanotubes. The specific molecular

(25) (a) von Kiedrowski, G. *Bioorg. Chem. Front.* **1993**, *3*, 113−146. (b) Luther, A.; Brandsch, R.; von Kiedrowski, G. *Nature* **1998**, *396*, 245−248. (c) Zielinski, W. S.; Orgel, L. E. *Nature* **1987**, *327*, 346−347. (d) Morgan, M. M.; Rebek, J., Jr. *Curr. Opin. Struct. Biol.* **1994**, *4*, 629−635. (e) Reinhoudt, D. N.; Rudkevitch, D. M.; de Jong, F. *J. Am. Chem. Soc.* **1996**, *118*, 6880−6889. (f) Joyce, G. F.; Orgel, L. E. *Cold Spring Harbor Monogr. Ser.* **1999**, *37*, 49−77. (g) Li, T.; Nicolaou, K. C. *Nature* **1994**, *369*, 218−221. (h) Saghatelian, A.; Yokobayashi, Y.; Soltani, K.; Ghadiri, M. R. *Nature* **2001**, *409*, 797−801. (i) Isaac, R.; Ham, Y.-W.; Chmielewski, J. A. *Curr. Opin. Struct. Biol.* **2001**, *11*, 458−463.
(26) (a) Prusiner, S. B.; Scott, M. R.; DeArmond, S. J.; Carlson, G. *Cold Spring Harbor Monogr. Ser.* **1999**, *38*, 147−190. (b) Masel, J.; Vincent, A. A.; Nowak, M. A. *Biophys. Chem.* **1999**, *77*, 139−152.

recognition of a chiral amino acid in its zwitterionic form (promoter) by **1** within the nanotubes results in an instantaneous transition from racemic to homochiral helical nanotubes according to the proposed scheme of Figure 11. Despite the polydispersity of the sample, the system displays an all-or-none chiroptical output depending on whether all of the crown ether sites of **1** within the nanotube are fully or partially occupied with a promoter. At micromolar concentrations, where **1** exists mainly in the nonassembled state, the promoter triggers a sequence of supramolecular reactions leading to the chirogenesis of helical rosette nanotubes with predefined helicities. This pathway involves a multicomponent, stereospecific, and hierarchical cascade of supramolecular reactions requiring first a molecular recognition event between **1** and L-Ala, followed by self-assembly into helical rosette nanotubes. Finally, depending on its concentration, a promoter can display a dominant or recessive behavior with respect to its supramolecular chirality output.

The strategies presented here may also be viewed as a process by which a predefined set of physical and chemical properties is expressed at the macromolecular level through a stereospecific, programmable, and potentially autocatalytic sequence of supramolecular reactions. We envision, as a result, numerous applications in adaptive chemistry,[27] dynamic combinatorial chemistry,[28] materials sciences,[29] and in the above-discussed areas of chirotechnology.[3a−d,8−13]

Acknowledgment. We thank Dr. Jaby Jacob and Dr. P. Thiyagarajan (Argonne National Laboratory) for the SAXS measurements and the Purdue Laboratory for Chemical Nanotechnology for technical support and expert advice. We acknowledge the support of the National Science Foundation (Career award), the American Cancer Society (ACS-IRG 58), the American Chemical Society (ACS-PRF), the Showalter Foundation, the 3M Company, and Purdue University. H.F. is a Cottrell Scholar of Research Corp.

Supporting Information Available: Materials and methods for CD, DLS, SAXS, TEM, and modeling studies. Representative Guinier plots and additional TEM micrographs (PDF). This material is available free of charge via the Internet at http://pubs.acs.org.

JA026164S

(27) Fernandez-Lopez, S.; Kim, H.-S.; Choi, E. C.; Delgado, M.; Granja, J. R.; Khasanov, A.; Kraehenbuehl, K.; Long, G.; Weinberger, D. A.; Wilcoxen, K. M.; Ghadiri, M. R. *Nature* **2001**, *412*, 452−456.
(28) (a) Lehn, J.-M.; Eliseev, A. V. *Science* **2001**, *291*, 231−232. (b) Sanders, J. K. M. *Pure Appl. Chem.* **2000**, *72*, 2265−2274. (c) Linton, B.; Hamilton, A. D. *Chem. Rev.* **1997**, *97*, 1669−1680. (d) Moore, J. S.; Zimmerman, N. W. *Org. Lett.* **2000**, *2*, 915−918. (e) Karan, C.; Miller, B. L. *DDT* **2000**, *5*, 67−75.
(29) Hartgerink, J. D.; Zubarev, E. R.; Stupp, S. I. *Curr. Opin. Solid State Mater. Sci.* **2001**, *5*, 355−361.